Characterization of Cytochrome *c* Membrane-binding Site Using Cardiolipin-containing Bicelles with NMR

Hisashi Kobayashi, Satoshi Nagao*, and Shun Hirota*

Abstract: Cytochrome (cyt) *c* transports electrons from Complex III to Complex IV in mitochondria. Cyt *c* is ordinarily anchored to the mitochondrial membrane by interaction with cardiolipin (CL), however its release to cytosol initiates apoptosis. Herein, the cyt *c* interaction site with CL-containing bicelles is characterized by NMR spectroscopy. Chemical shift perturbations in cyt *c* signals by interaction with bicelles revealed that a relatively wide region, including the A-site, CXXCH motif, and N- and C-terminal helices, with multiple Lys residues, interacts cooperatively with CL. The specific cyt *c*−CL interaction strengthened with increasing CL molecules in the bicelles. The cyt *c* interaction site with CL was similar to those with Complex III and Complex IV, indicating that cyt *c* recognizes lipids and partner proteins in a similar way. In addition to elucidating the cyt *c* membrane-binding site, these results provide a dynamic aspect of cyt *c* for interaction with molecules in mitochondria.

Membrane proteins associated with lipid molecules play diverse roles in cells. The roles include immunoreaction in innate immunity,[1] molecular and ion transportation across cell membranes,[2] and ATP synthesis in the respiratory chain.[2b, 3] Lipid molecules serve not only as scaffolds but also regulatory factors of membrane proteins in biological systems.[4] Cytochrome (cyt) *c* is a peripheral membrane protein which shuttles electrons from the cyt bc_1 complex (Complex III) to cyt *c* oxidase (Complex IV) in the respiratory chain.[5] Cyt *c* is ordinarily anchored to the inner mitochondrial membrane by binding to cardiolipin (CL), a specific glycerophospholipid.[6]

Although there have been many studies on the binding character of cyt *c* to CL-containing membranes,[6-7] the CL-interaction sites of cyt *c* have lacked high resolution. Spherical vesicles comprising amphipathic phospholipids have been typically used as membrane mimetics to elucidate cyt *c*−lipid interactions.[6, 7c-e] NMR spectroscopy can provide us detailed structural information on interactions of proteins with other molecules.[8] However, for protein−vesicle systems, the tumbling motion of the protein is slowed down by binding to the vesicle causing signal broadening in solution, since the molecular weights of the vesicles are well above the molecular weight limit of NMR signal detection for conventional structural characterization (about 100 kDa).[9] Small detergent micelles have been used for characterization of protein−lipid interactions by solution NMR spectroscopy, although a conceivable effect of the micelle curvature on the protein structure remains a concern.[8b, 10] Recently, CL-bound cyt *c* was encapsulated into a reversed-micelle in organic solvents and characterized by solution NMR spectroscopy, where cyt *c* interacted with the membrane mimetics possessing a large negative curvature.[8e] Disk-like bicelles are constructed of short- and long-chain lipids, which are separated in rim and bilayer phases, respectively.[11] Bicelles have been utilized to obtain structural and functional insights on membrane proteins by combination with solution and solid-state NMR spectroscopies.[8b, 12] Small bicelles tumble quickly in solution at an NMR time scale, allowing solution NMR investigation of the interaction between a peripheral membrane protein and a bicelle containing lipids which interact with the protein. Nanodiscs formed by a mixture of lipids and membrane scaffold proteins have been developed to characterize membrane proteins in an aqueous medium.[13] In this study, we used bicelles with a limited number of CL in each bicelle to characterize the interaction of horse cyt *c* with CL by high-resolution solution NMR spectroscopy.

The bicelle structure and size were characterized by ^{31}P NMR, cryogenic transmission electron microscopy (Cryo-TEM), and dynamic light scattering (DLS). In the ^{31}P NMR spectra of the bicelles, three narrow signals corresponding to the phosphate groups of 1,2-dihexanoyl-*sn*-glycero-3-phosphocholine (DHPC), 1,2-dimyristoyl-*sn*-glycero-3-phosphocholine (DMPC), and bovine heart CL were all observed between −1.0 and 1.0 ppm (**Figure 1A**). The DHPC and DMPC chemical shifts of the bicelles were similar to those previously reported for DHPC/DMPC bicelles, which exhibited isotropic tumbling motions in solution.[12b] Line broadening of the CL signal in the ^{31}P NMR spectra was similar to those of other signals (**Table S1**), indicating that CL was incorporated into the bicelles. The bicelles of DHPC:DMPC:CL = 1:0.9:0.1, 1.33:0.9:0.1, and 2:0.9:0.1 (molar ratio) were estimated to form q=1, q=0.75, and q=0.5 (ratio of long-chain to short-chain components) bicelles, respectively, by assuming that DHPC formed the rim region whereas DMPC and CL formed the lipid bilayer region. The bicelles contained 10 mol% CL in their lipid bilayer regions. The linewidths of the ^{31}P signals in the spectra increased in the order of the q value, corresponding to the increase in the bicelle size (**Figure 1A**). However, the ^{31}P NMR spectra of the bicelles did not change with an addition of cyt *c*, indicating that the bicelles maintained their structures in the presence of cyt *c* (**Figure S1**). Ellipsoidal objects corresponding to the projections of edge-on discoidal structures were observed in the cryogenic transmission electron microscopy (Cryo-TEM) image of the q=1 bicelles (**Figure S2**). Average sizes of q=1, q=0.75, and q=0.5 bicelles were estimated by DLS as (9.14 ± 0.81) nm, (6.74 ± 0.24) nm, and (4.73 ± 0.16) nm with half widths of 2.70 nm, 1.81 nm, and 1.23 nm, respectively (**Figure 1B**).

[*] H. Kobayashi, Dr. S. Nagao, Prof. Dr. S. Hirota
Graduate School of Materials Science
Nara Institute of Science and Technology
8916-5 Takayama, Ikoma, Nara 630-0192, Japan
E-mail: s-nagao@ms.naist.jp, hirota@ms.naist.jp

Supporting information for this article is given via a link at the end of the document.

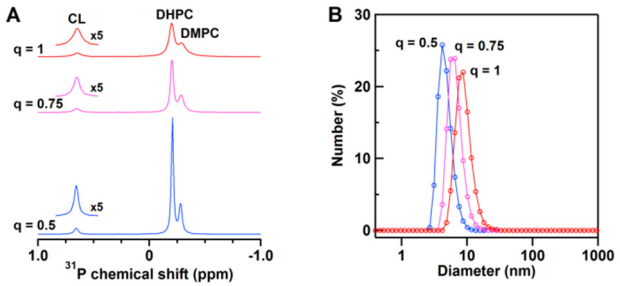

Figure 1. (A) ^{31}P NMR spectra and (B) DLS size distribution curves of CL-containing bicelles. The spectra and curves for the q=1, q=0.75, and q=0.5 bicelles are shown in red, pink, and blue, respectively. Measurement conditions: solution condition, 25 mM HEPES-NaOH buffer, pH 6.8, containing 50 mM NaCl; [DHPC], 30, 40, and 60 mM for the q=1, q=0.75, and q=0.5 bicelles, respectively; [DMPC], 27 mM; [CL], 3 mM; temperature, 25 ºC.

^{1}H and ^{15}N signals of backbone amino acid residues except Gly1, Glu21, Thr28, Pro30, Gly37, Pro44, Gly45, Thr47, Pro71, Pro76, Gly77, Ala83, Gly84, Lys86, and Lys88 of oxidized wild-type (WT) cyt *c* were assigned, and the chemical shifts of the signals were in good agreement with those reported previously.[8e, 14]

Solution NMR spectra of oxidized cyt *c* were compared in the presence and absence of CL-containing bicelles to elucidate the interactions between cyt *c* and CL. The linewidths of the ^{1}H NMR signals of WT cyt *c* increased slightly by an addition of q=1 bicelles containing CL (**Figure S3B**), whereas it did not change by an addition of q=1 bicelles not containing CL (**Figure S3C**). These results indicated that WT cyt *c* interacted with CL in the bicelles. However, in the presence of CL-containing 1,2-dioleoyl-*sn*-glycero-3-phosphocholine (DOPC) vesicles, most of the ^{1}H NMR signals of WT cyt *c* were undetectable by severe signal broadening, due to the large molecular weight of the vesicles (**Figure S3D**).

The chemical shift perturbation (CSP) values of Asp2, Lys5, Gly6, Lys7, Lys8, Gln16, Glu61, Glu62, Lys87, and Thr89 of WT cyt *c* by the addition of CL-containing q=1 bicelles were larger than the average CSP value of all residues for more than the standard deviation (large CSP: CSP value ≧ 0.014 ppm) (**Figures 2 and S4**). The CSP values of Val3, Ile9, Gln12, Lys13, Cys17, His18, Thr19, Val20, Gly29, Ala51, Asn54, Asn70, Lys72, Lys73, Tyr74, Phe82, Ile85, Arg91, Asp93, Leu94, Tyr97, and Leu98 were larger than the average CSP value, but within the standard deviation (moderate CSP: 0.008 ppm < CSP value < 0.014 ppm). CSP is caused by the change in the magnetic shielding, due to a contact with opponents and/or a local protein conformational change.[8a] The amino acid residues of cyt *c* in a specific surface region containing multiple Lys residues (Lys5, Lys7, Lys8, Lys13, Lys72, Lys73, and Lys87) exhibited large or moderate CSP values, revealing that this region was involved in the interaction with CL in the q=1 bicelle (**Figure 2B**).

The effect of the number of CL molecules in the bicelle on the cyt *c*−CL interaction was investigated with q=0.75 and q=0.5 bicelles containing CL. Although it seems convenient to use q=1 bicelles with different CL/DMPC ratios for elucidation of the effect of CL amount in a bicelle, the preparation of low CL content bicelles was difficult due to the low solubility of the lipids (e.g. 600 mM of lipids was required for preparation of q=1 bicelles containing 1 mol% CL in the lipid bilayer region). Additionally, aggregates were obtained by interaction of cyt *c* with lipids for the q=1 bicelles containing 20 mol% CL in the lipid bilayer region. Thus, we constructed q=0.75 and q=0.5 bicelles containing 10 mol% CL in the lipid bilayer regions, and varied the number of CL molecules in the bicelle by changing the bicelle size. The number of CL molecules in a bicelle was calculated as 25, 12, and 4 for the q=1, q=0.75, and q=0.5 bicelles, respectively (half of the CL molecules were estimated to exist in each side of the bicelle), assuming a homogenous distribution and using the lipid molecular volumes.[15] Although the CL density of the lipid bilayer was the same among different q-value bicelles, a cyt *c* molecule may interact with more CL molecules within a bicelle when the bicelle contains more CL molecules (**Figure S5**). The CSP values of cyt *c* associated with the addition of CL-containing q=0.75 and q=0.5 bicelles increased by increasing the number of CL molecules in the bicelles, although the cyt *c*/CL and CL/DMPC ratios were the same (**Figures 2A and S5**). These results show that the specific interaction of cyt *c* with CL became stronger with the increase in the number of CL molecules in the bicelles. It is noteworthy that the cyt *c*−CL interaction was weak for the q=0.5 bicelle, even though the CL density of the bicelle was the same as that of the q=1 bicelle.

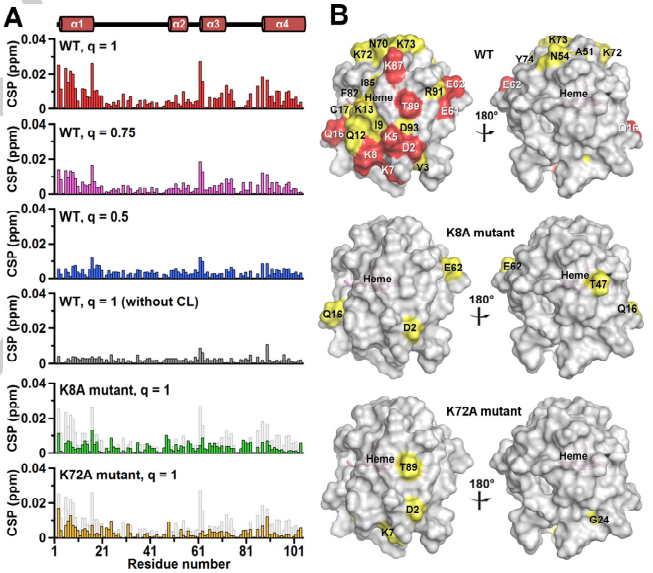

Figure 2. CSP values of the amino acid residues and surface mapping of oxidized WT, K8A, and K72A cyt *c* in the presence of CL-containing bicelles. (A) The CSP values of backbone signals induced by the interaction with CL are represented in bars. The chemical shift changes of WT cyt *c* for the q=1, q=0.75, and q=0.5 bicelles with CL are shown in red, pink, and blue, respectively. The CSP values of WT cyt *c* for the q=1 bicelle without CL are shown in dark gray. The CSP values of WT cyt *c* are superimposed as light gray bars to those of K8A (green) and K72A (orange) cyt *c*. (B) The protein structure (PDB: 1AKK) is shown in surface models. The residues with CSP values of x < 0.008, 0.008 ≦ x < 0.014, and 0.014 ≦ x are shown in gray, yellow, and red, respectively. The heme positions are shown in purple. The left and right figures are rotated horizontally 180º. Measurement conditions: solution condition, 25 mM HEPES-NaOH buffer, pH 6.8, containing 50 mM NaCl; [cyt *c*], 0.3 mM; [DHPC], 30, 40, and 60 mM for the q=1, q=0.75, and q=0.5 bicelles, respectively; [DMPC], 27 mM; [CL], 3 mM; [K_3[Fe(CN)$_6$]], 0.3 mM; temperature, 25 ºC.

To elucidate whether the amino acid residues in the specific surface region interacted with CL independently or cooperatively, we separately replaced two positively charged Lys residues which exhibited substantial CSP (Lys8 and Lys72) to Ala (**Figure S6**)—the two Lys residues were located on the opposite sides of the CL-interaction site (**Figure 2B**) (distance between the C_β carbons is ~2.6 nm)—and elucidated their effects on the CL-interaction site using the q=1 bicelle. The CSP values associated with the addition of the q=1 bicelles containing CL decreased significantly by the replacement of Lys8 or Lys72 (**Figure 2**). Since Lys8 and Lys72 were relatively distant, these results indicated that the Lys residues in the specific region interacted cooperatively with CL.

From the bicelle size and volumes of the lipid compositions, the molecular weights of the bicelles were estimated to be about 300, 150, and 60 kDa for the q=1, q=0.75, and q=0.5 bicelles, respectively.[15] Considering that the molecular weight limit of conventional NMR structural characterization in solution NMR spectroscopy,[8b] the high-resolution structural analysis of these bicelles seems difficult. However, the backbone signals of cyt *c* in the presence of CL-containing q=1 and q=0.75 bicelles were broadened only slightly in the solution NMR spectra (**Figure S3B and Table S1**), and the CSP values of the amino acid residues were successfully detected (**Figure 2**). Under the present cyt *c* and CL-containing bicelle concentrations, only a certain amount of cyt *c* molecules may have existed in the CL-bound state, whereas the rest existed in the free state, and the two states exchanged between each other during the signal detection, i.e., fast or intermediate exchange existed at NMR time scale. Additionally, the high dynamic mobility of the molecules in the bicelle may have contributed to the decrease in the NMR signal linewidths.[16]

The structure of membrane proteins and the interaction between membrane proteins and lipids have gained much attention in terms of understanding various biological events in organisms. The CL-interaction site of cyt *c* has been proposed by studies using CL-containing vesicles (**Figure S7A**). For example, the A-site containing Lys72, Lys73, Lys86, and Lys87 and the C-site containing Asn52 have been reported as a high-affinity electrostatic site[6b] and a low-affinity hydrophobic site,[6a] respectively. The CL binding at the C-site has been suggested to accommodate a hydrophobic channel for the insertion of the CL acyl-chain, leading to dissociation of Met80 from the heme iron.[17] The L-site containing Lys22, Lys25, His26, Lys27, and His33 is an electrostatic interaction site for the acidic phospholipids at low pH, where the membrane fusion is facilitated by the binding at this site.[7c] By CSP analysis, the A- and L-sites have been reported as the binding sites for reversed-micelles containing CL in organic solvents.[8e] In the present study, the A-site was identified as the reversible binding site of cyt *c* in the CL-containing q=1 bicelles (although no signal was detected for Lys86 in the NMR spectra) (**Figure 2B**), whereas the C- and L-sites were not identified as the interaction site. When cyt *c* interacted with the CL-containing q=1 bicelles, Met80 dissociation from the heme iron did not occur, since the Soret band and 695-nm absorption band did not change significantly, by the interaction with the bicelles (**Figure S8**). Given these results, we propose that the interaction of cyt *c* with CL at the A-site is established prior to the irreversible binding at the C-site.

In addition to the residues at the A-site, the residues at the N-terminal helix, CXXCH motif, and the C-terminal helix (Asp2, Val3, Lys5, Lys7, Lys8, Ile9, Gln12, Lys13, Asn16, Cys17, Ile85, Thr89, Asp93) of horse cyt *c* were included in the interaction site with the CL-containing q=1 bicelles, forming a relatively wide region (**Figures 2B** and **S7B**). Notably, this wide region corresponded well to the cyt *c* interaction site for its redox partners, Complex III[5e] and Complex IV[8a] (**Figure 3**). According to the high-resolution structure of iso-1 cyt *c* bound to Complex III revealed by X-ray crystallographic analysis, the residues (Lys11, Thr12, Arg13, Gln16, Lys27, Val28, Ala81, Gly83, Lys86, Lys87, and Lys89, in horse numbering) near the interface of N- and C-terminal helices of iso-1 cyt *c* interact with Complex III.[5e] The interaction site of oxidized human cyt *c* with Complex IV has been revealed by solution NMR spectroscopy, where Asp2, Lys5, Ile9, Ile11 (Val in horse cyt *c*), Met12 (Gln in horse cyt *c*), Lys13, Ser15 (Ala in horse cyt *c*), Cys17, His18, Lys79, Met80, Ile81, Val83 (Ala in horse cyt *c*), Lys86, Lys87, Lys88, Glu89 (Thr in horse cyt *c*), Glu90, and Asp93 exhibited large CSP values.[8a] The similarity among the interaction sites of cyt *c* with CL, Complex III, and Complex IV reveals that cyt *c* recognizes the lipids and its partner proteins at a similar site, and may exchange its partner by sliding on the inner mitochondrial membrane.

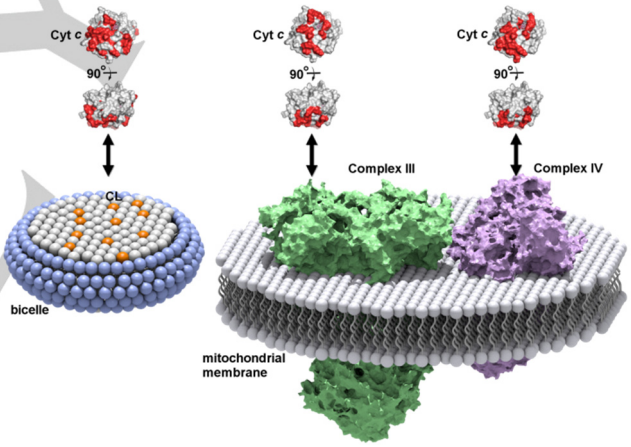

Figure 3. Schematic diagram of cyt *c* interaction sites with a CL-containing bicelle, Complex III, and Complex IV. The interaction sites of cyt *c* (PDB:1AKK) for CL (present work), Complex III,[5e] and Complex IV[8a] are shown in red. The head groups of the lipid molecules are shown as sphere models. DHPC, DMPC, and CL molecules in the bicelle are shown in blue, gray, and orange, respectively. Complex III, and Complex IV are shown in green and purple, respectively.

In conclusion, we identified a relatively wide CL-interaction site for cyt *c* by solution NMR spectroscopy using CL-containing bicelles. The site contained the well-known A-site, N-terminal helix, CXXCH motif, and C-terminal helix, with multiple Lys residues interacting cooperatively with CL. Application of bicelles for the characterization of protein−lipid interaction with high-resolution solution NMR spectroscopy may provide us new insights on not only the detailed interaction sites of peripheral membrane proteins but also their dynamics at the membrane surface.

Acknowledgements

We thank Ms. Yukie Kitada for preliminary experiments. We are also grateful to Mr. Leigh McDowell (Nara Institute of Science and Technology) for his advice on manuscript preparation. This work was partially supported by Grants-in-Aid from JSPS for Young Scientists (B) (No. JP24750163 (S.N.)) and Scientific Research (B) (No. JP26288080 (S.H.))). This study was also supported by the Green Photonics Project at NAIST sponsored by MEXT.

Keywords: cytochrome *c* • cardiolipin • protein-lipid interaction • bicelle • solution NMR

[1] C. A. Janeway, Jr., R. Medzhitov, *Annu. Rev. Immunol.* **2002**, *20*, 197-216.

[2] a) K. S. Ullman, M. A. Powers, D. J. Forbes, *Cell* **1997**, *90*, 967-970; b) K. Faxén, G. Gilderson, P. Ädelroth, P. Brzezinski, *Nature* **2005**, *437*, 286-289; c) A. L. Stouffer, R. Acharya, D. Salom, A. S. Levine, L. Di Costanzo, C. S. Soto, V. Tereshko, V. Nanda, S. Stayrook, W. F. DeGrado, *Nature* **2008**, *451*, 596-599.

[3] M. Yoshida, E. Muneyuki, T. Hisabori, *Nat. Rev. Mol. Cell Biol.* **2001**, *2*, 669-677.

[4] a) O. S. Andersen, R. E. Koeppe, II, *Annu. Rev. Biophys. Biomol. Struct.* **2007**, *36*, 107-130; b) R. Phillips, T. Ursell, P. Wiggins, P. Sens, *Nature* **2009**, *459*, 379-385.

[5] a) S. J. Singer, *Annu. Rev. Biochem.* **1974**, *43*, 805-833; b) B. E. Ramirez, B. G. Malmström, J. R. Winkler, H. B. Gray, *Proc. Natl. Acad. Sci. U.S.A.* **1995**, *92*, 11949-11951; c) H. Witt, F. Malatesta, F. Nicoletti, M. Brunori, B. Ludwig, *Eur. J. Biochem.* **1998**, *251*, 367-373; d) N. V. Dudkina, H. Eubel, W. Keegstra, E. J. Boekema, H.-P. Braun, *Proc. Natl. Acad. Sci. U.S.A.* **2005**, *102*, 3225-3229; e) S. R. N. Solmaz, C. Hunte, *J. Biol. Chem.* **2008**, *283*, 17542-17549; f) T. Althoff, D. J. Mills, J.-L. Popot, W. Kühlbrandt, *EMBO J.* **2011**, *30*, 4652-4664.

[6] a) M. Rytömaa, P. K. Kinnunen, *J. Biol. Chem.* **1994**, *269*, 1770-1774; b) M. Rytömaa, P. K. Kinnunen, *J. Biol. Chem.* **1995**, *270*, 3197-3202.

[7] a) M. Ott, J. D. Robertson, V. Gogvadze, B. Zhivotovsky, S. Orrenius, *Proc. Natl. Acad. Sci. U.S.A.* **2002**, *99*, 1259-1263; b) V. E. Kagan, V. A. Tyurin, J. Jiang, Y. Y. Tyurina, V. B. Ritov, A. A. Amoscato, A. N. Osipov, N. A. Belikova, A. A. Kapralov, V. Kini, I. I. Vlasova, Q. Zhao, M. Zou, P. Di, D. A. Svistunenko, I. V. Kurnikov, G. G. Borisenko, *Nat. Chem. Biol.* **2005**, *1*, 223-232; c) C. Kawai, F. M. Prado, G. L. Nunes, P. Di Mascio, A. M. Carmona-Ribeiro, I. L. Nantes, *J. Biol. Chem.* **2005**, *280*, 34709-34717; d) N. A. Belikova, Y. A. Vladimirov, A. N. Osipov, A. A. Kapralov, V. A. Tyurin, M. V. Potapovich, L. V. Basova, J. Peterson, I. V. Kurnikov, V. E. Kagan, *Biochemistry* **2006**, *45*, 4998-5009; e) L. V. Basova, I. V. Kurnikov, L. Wang, V. B. Ritov, N. A. Belikova, Vlasova, II, A. A. Pacheco, D. E. Winnica, J. Peterson, H. Bayir, D. H. Waldeck, V. E. Kagan, *Biochemistry* **2007**, *46*, 3423-3434; f) P. A. Beales, C. L. Bergstrom, N. Geerts, J. T. Groves, T. K. Vanderlick, *Langmuir* **2011**, *27*, 6107-6115; g) Y. Hong, J. Muenzner, S. K. Grimm, E. V. Pletneva, *J. Am. Chem. Soc.* **2012**, *134*, 18713-18723; h) J. Hanske, J. R. Toffey, A. M. Morenz, A. J. Bonilla, K. H. Schiavoni, E. V. Pletneva, *Proc. Natl. Acad. Sci. U.S.A.* **2012**, *109*, 125-130.

[8] a) K. Sakamoto, M. Kamiya, M. Imai, K. Shinzawa-Itoh, T. Uchida, K. Kawano, S. Yoshikawa, K. Ishimori, *Proc. Natl. Acad. Sci. U.S.A.* **2011**, *108*, 12271-12276; b) U. H. N. Dürr, M. Gildenberg, A. Ramamoorthy, *Chem. Rev.* **2012**, *112*, 6054-6074; c) R. E. McGovern, H. Fernandes, A. R. Khan, N. P. Power, P. B. Crowley, *Nat. Chem.* **2012**, *4*, 527-533; d) C. O'Connor, K. L. White, N. Doncescu, T. Didenko, B. L. Roth, G. Czaplicki, R. C. Stevens, K. Wüthrich, A. Milon, *Proc. Natl. Acad. Sci. U.S.A.* **2015**, *112*, 11852-11857; e) E. S. O'Brien, N. V. Nucci, B. Fuglestad, C. Tommos, A. J. Wand, *J. Biol. Chem.* **2015**, *290*, 30879-30887; f) A. Mandal, C. L. Hoop, M. DeLucia, R. Kodali, V. E. Kagan, J. Ahn, P. C. A. van der Wel, *Biophys. J.* **2015**, *109*, 1873-1884.

[9] G. Wang, *Curr. Prot. Pept. Sci.* **2008**, *9*, 50-69.

[10] E. Bárány-Wallje, A. Andersson, A. Gräslund, L. Mäler, *FEBS Lett.* **2004**, *567*, 265-269.

[11] C. R. Sanders, II, G. C. Landis, *Biochemistry* **1995**, *34*, 4030-4040.

[12] a) K. J. Glover, J. A. Whiles, G. Wu, N. Yu, R. Deems, J. O. Struppe, R. E. Stark, E. A. Komives, R. R. Vold, *Biophys. J.* **2001**, *81*, 2163-2171; b) M. N. Triba, D. E. Warschawski, P. F. Devaux, *Biophys. J.* **2005**, *88*, 1887-1901; c) E. A. Morrison, G. T. DeKoster, S. Dutta, R. Vafabakhsh, M. W. Clarkson, A. Bahl, D. Kern, T. Ha, K. A. Henzler-Wildman, *Nature* **2012**, *481*, 45-50.

[13] T. H. Bayburt, Y. V. Grinkova, S. G. Sligar, *Nano Lett.* **2002**, *2*, 853-856.

[14] L. Banci, I. Bertini, H. B. Gray, C. Luchinat, T. Reddig, A. Rosato, P. Turano, *Biochemistry* **1997**, *36*, 9867-9877.

[15] R. S. Armen, O. D. Uitto, S. E. Feller, *Biophys. J.* **1998**, *75*, 734-744.

[16] J. Dittmer, L. Thøgersen, J. Underhaug, K. Bertelsen, T. Vosegaard, J. M. Pedersen, B. Schiøtt, E. Tajkhorshid, T. Skrydstrup, N. C. Nielsen, *J. Phys. Chem. B* **2009**, *113*, 6928-6937.

[17] F. Sinibaldi, B. D. Howes, M. C. Piro, F. Polticelli, C. Bombelli, T. Ferri, M. Coletta, G. Smulevich, R. Santucci, *J. Biol. Inorg. Chem.* **2010**, *15*, 689-700.

Entry for the Table of Contents (Please choose one layout)

Protien–Membrane Interaction

COMMUNICATION

Molecular recognition: Cytochrome (cyt) *c* interaction site with cardiolipin (CL)-containing bicelles was characterized by solution NMR spectroscopy. Chemical shift perturbations in cyt *c* signals by interaction with bicelles revealed that the cyt *c* interaction site with CL was similar to those with Complex III and Complex IV.

.

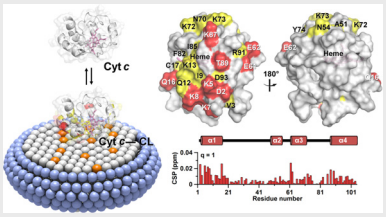

Hisashi Kobayashi, Satoshi Nagao, and Shun Hirota**

Page No. – Page No.

Characterization of Cytochrome *c* Membrane-binding Site Using Cardiolipin-containing Bicelles with NMR

Contents

Experimental Section

Preparation of bicelles. DHPC and bovine heart CL were purchased from Avanti Polar Lipids (Alabaster, USA). DMPC and DOPC were purchased from NOF corporation (Tokyo, Japan). The lipid mixtures of DHPC:DMPC:CL = 1:0.9:0.1, 1.33:0.9:0.1, and 2:0.9:0.1 (molar ratio) were dissolved in chloroform and dried up by solvent evaporation to form film-like lipid mixtures. The obtained lipid mixture was suspended in 25 mM HEPES-NaOH buffer, pH 6.8, containing 50 mM NaCl, and repeatedly frozen and thawed four times to homogenize the lipid mixture. A lipid mixture not containing CL was prepared by the same procedure. The molar ratio of long-chain phospholipid to short-chain phospholipid ([DMPC]+[CL])/[DHPC] or [DMPC]/[DHPC]) is denoted as q. The DOPC vesicle containing CL was prepared from the lipid mixture with a DOPC:CL molar ratio of 0.9:0.1 by the same procedure. To adjust the size of the vesicles, the vesicles were passed through a 50 nm polycarbonate membrane 15 times using a LiposoFast-Extruder (Avestin, Ottawa, ON, Canada).

Preparation of ^{15}N-labeled cyt *c*. Oligonucleotide primers were purchased from Sigma-Aldrich Japan (Tokyo, Japan). The DNA sequence of the plasmid coding the human cyt *c* gene was converted to the horse cyt *c* gene by PCR-based mutagenesis with the KOD Plus Mutagenesis kit (Toyobo, Osaka, Japan) using four sets of forward and reverse primers (**Table S2**).[1] K8A and K72A horse cyt *c* mutant genes were constructed from the horse WT cyt *c* gene with HH-K8A-F and HH-K8A-R primers and HH-K72A-F and HH-K72A-R primers, respectively (**Table S2**). The gene sequences were confirmed by DNA sequencing (ABI 3100 Avant generic analyzer, Applied Biosystems, Inc., Foster City, USA) with the BigDye Terminator v3.1 cycle sequencing kit (Applied Biosystems, Inc.). The non-labeled recombinant horse cyt *c* was expressed in *Escherichia coli* (*E. coli*) with a similar method as reported previously.[1] *E. coli* was grown in M9 minimum medium[2] with $^{15}NH_4Cl$ to obtain ^{15}N-labeled recombinant proteins. Purification of the recombinant protein was performed according to a previously published method.[1] The solvent of the protein solution was exchanged with 25 mM HEPES-NaOH buffer, pH 6.8, containing 50 mM NaCl. Molar extinction coefficients of oxidized K8A and K72A cyt *c* proteins at 409 nm were determined by the hemochrome method[3] as $\varepsilon = 1.18 \times 10^5$ $M^{-1}cm^{-1}$ and $\varepsilon = 1.20 \times 10^5$ $M^{-1}cm^{-1}$, respectively. The horse cyt *c* concentration was adjusted by the Soret band intensity.

Nuclear magnetic resonance measurements. NMR measurements of q=1, q=0.75, and q=0.5 bicelles containing CL and oxidized horse *c* in the presence and absence of the bicelles were carried out with a JNM-ECA600 spectrometer (JEOL, Tokyo, Japan) at 25 ºC. ^{1}H, ^{15}N, and ^{31}P resonance frequencies were 600 MHz, 60.8 MHz, and 243 MHz, respectively. One dimensional NMR spectra were processed using the program Delta 5.0 (JEOL). Two and three dimensional

NMR spectra were processed using the NMR pipe program[4] and analyzed using the Sparky program (SPARKY 3, Goddard TD and Kneller DG, University of California, San Francisco, http://www.cgl.ucsf.edu/home/sparky/). Micro tube (BMS-005J, Shigemi, Tokyo, Japan) was used for all NMR measurements. ^{1}H and ^{15}N signals of backbone amino acid residues except Gly1, Glu21, Thr28, Pro30, Gly37, Pro44, Gly45, Thr47, Pro71, Pro76, Gly77, Ala83, Gly84, Lys86, and Lys88 of oxidized wild-type (WT) cyt *c* were assigned using three-dimensional ^{15}N-edited NOE correlated spectroscopy (NOESY)-heteronuclear single quantum coherence (HSQC) and totally correlated spectroscopy (TOCSY)-HSQC NMR spectra. The backbone ^{1}H-^{15}N signals of K8A and K72A cyt *c* mutants were also assigned by a similar procedure. Only small differences in the ^{1}H chemical shifts were observed between WT and mutant cyt *c* around the mutated positions (**Fig. S6**), indicating that the replacements of Lys8 and Lys72 with Ala did not affect the tertiary structure of cyt *c* significantly. The chemical shift perturbation (CSP) values were calculated from the chemical shift changes of the signals by the following equation.[5]

$$\text{CSP value} = \{\Delta\delta_H^2 + (\Delta\delta_N \times 0.154)^2\}^{1/2}$$

$\Delta\delta_H$ and $\Delta\delta_N$ represent the differences between the signals observed in the presence and absence of the bicelles for the ^{1}H and ^{15}N chemical shifts, respectively.

Dynamic light scattering measurements. Hydrodynamic diameter of q=1, q=0.75, and q=0.5 bicelles containing CL were measured at 25°C by a DLS spectrometer equipped with a He-Ne laser at 633 nm (Zetasizer Nano-ZS, Malvern, Malvern, UK). Number distribution of the lipid mixture was obtained by analyzing the time course of the scattering light intensity at an angle of 173° from the incident light with the Cumulant method.

Cryo-transmission electron microscope observation. A 200 mesh copper grid (JEOL, Tokyo, Japan) was pre-treated with a glow-discharger (HDT-400, JEOL) to obtain a hydrophilic surface. The q=1 bicelles containing CL (total lipid concentration; 60 mM) were placed on the copper grid and immediately plunged into liquid propane using a specimen preparation machine (EM-CPC, Leica, Wetzlar, Germany). The temperature was maintained lower than -140 °C by a cryotransfer holder (Model 626.DH, Gatan, Pleasanton, USA) during the observation. Microscopic observation was carried out using a transmission electron microscope (JEM-3100FEF, JEOL) at an acceleration voltage of 300 kV on zero-loss imaging mode.

Optical absorption measurements. Absorption spectra of 0.3 mM oxidized cyt *c* were measured with a UV-2450 spectrophotometer (Shimadzu, Kyoto, Japan) using a 0.1 or 1 mm path-length quartz cell at 25°C.

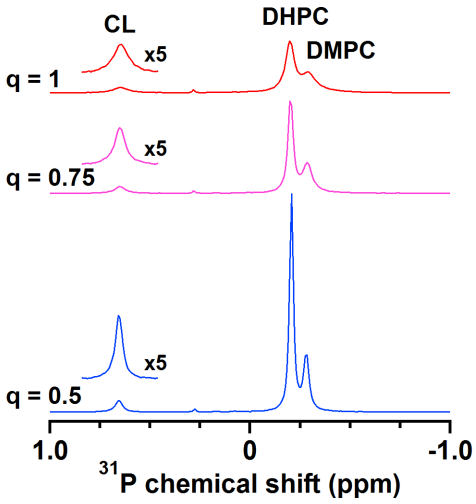

Fig. S1. ^{31}P NMR spectra of CL-containing bicelles after incubation with oxidized WT cyt *c* for 12 h. The spectra were measured in the presence of WT cyt *c*. The spectra of q=1, q=0.75, and q=0.5 bicelles are shown in red, pink, and blue, respectively. Measurement conditions: solution condition; 25 mM HEPES-NaOH, pH 6.8, containing 50 mM NaCl; [cyt *c*], 0.3 mM; [DHPC], 30, 40, and 60 mM for the q=1, q=0.75, and q=0.5 bicelles, respectively; [DMPC], 27 mM; [CL], 3 mM; [$K_3[Fe(CN)_6]$], 0.3 mM.

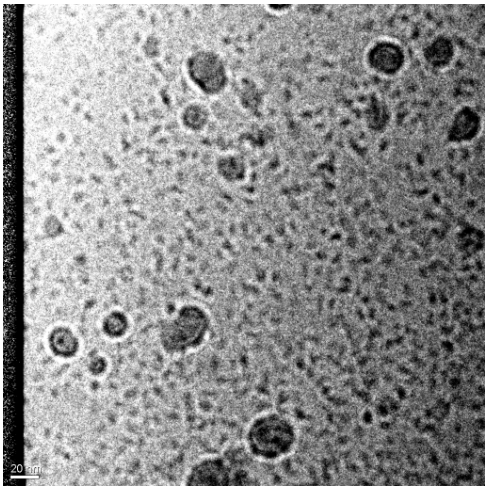

Fig. S2. Cryo-TEM image of CL-containing q=1 bicelles. Measurement conditions: solution condition; 25 mM HEPES-NaOH, pH 6.8, containing 50 mM NaCl; [DHPC], 30 mM; [DMPC], 27 mM; [CL], 3 mM; [$K_3[Fe(CN)_6]$], 0.3 mM.

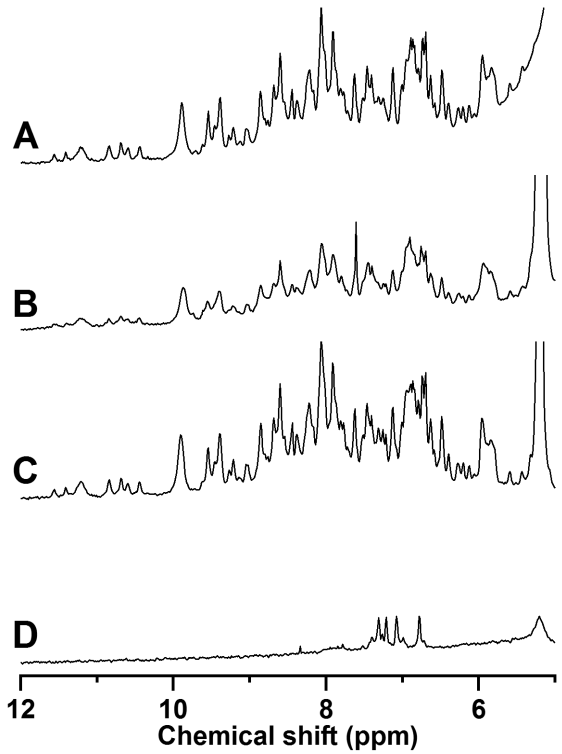

Fig. S3. The amide proton region of the ^{1}H NMR spectra of oxidized WT cyt *c* in the presence and absence of bicelles and vesicles. The spectra were observed (A) in the absence of lipid molecules and in the presence of (B) CL-containing q=1 bicelles, (C) q=1 bicelles not containing CL, and (D) CL-containing DOPC vesicles. Measurement conditions: solution condition; 25 mM HEPES-NaOH, pH 6.8, containing 50 mM NaCl; [cyt *c*], (A, B, C) 0.3 mM and (D) 0.1 mM; lipid concentrations, (B) [DHPC] (30 mM), [DMPC] (27 mM), [CL] (3 mM), (C) [DHPC] (30 mM), [DMPC] (30 mM), (D) [DOPC] (10 mM), [CL] (3 mM); [$K_3[Fe(CN)_6]$], (A, B, C) 0.3 mM and (D) 0.1 mM; temperature, 25 ºC.

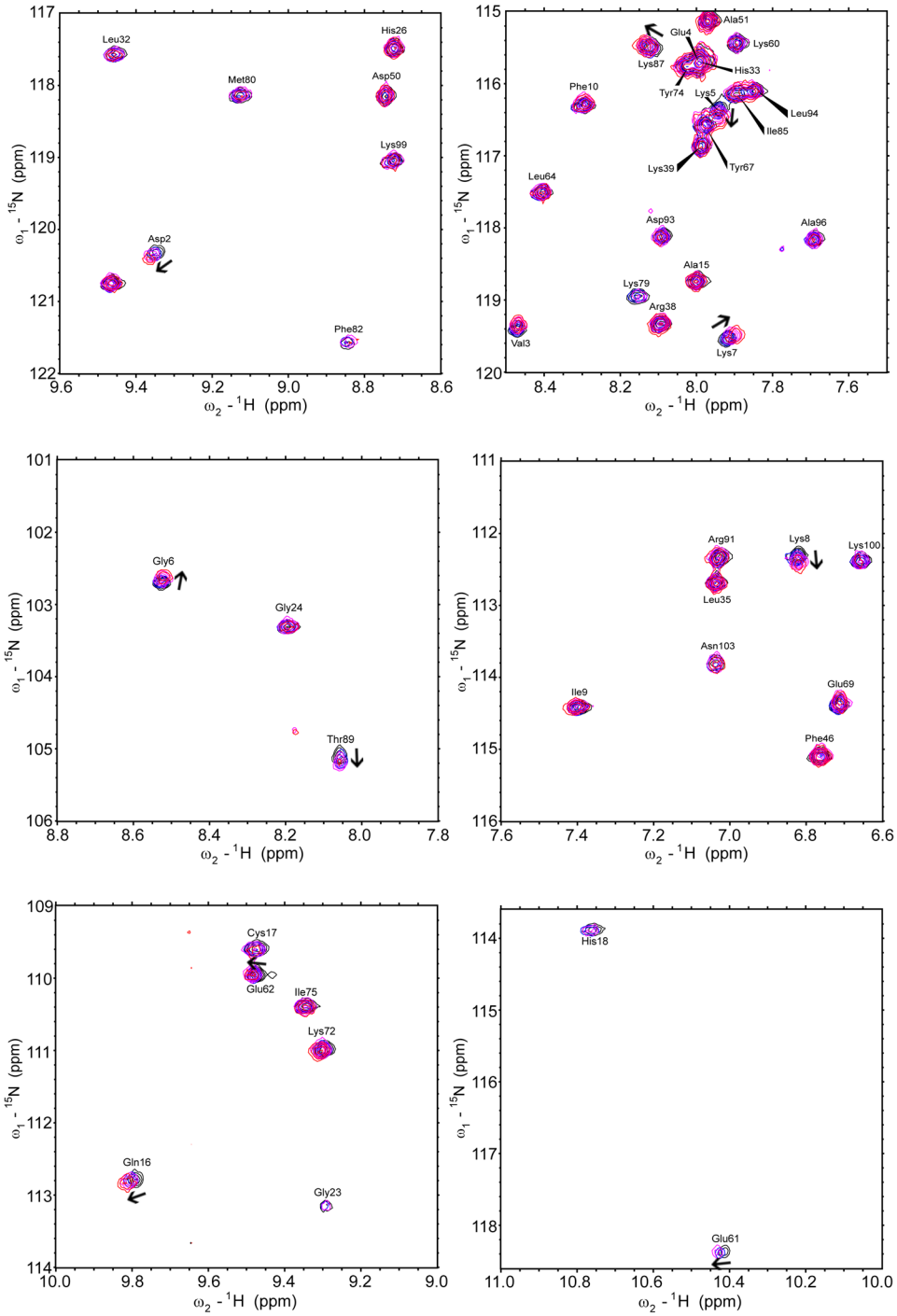

Fig. S4. Overlaid ^{1}H-^{15}N HSQC spectra of oxidized WT cyt *c* in the presence of q=1 (red), q=0.75 (pink), and q=0.5 (blue) CL-containing bicelles and in the absence of them (black). The chemical shift changes of Asp2, Lys5, Gly6, Lys7, Lys8, Gln16, Glu61, Glu62, Lys87, and Thr89 are indicated by arrows.

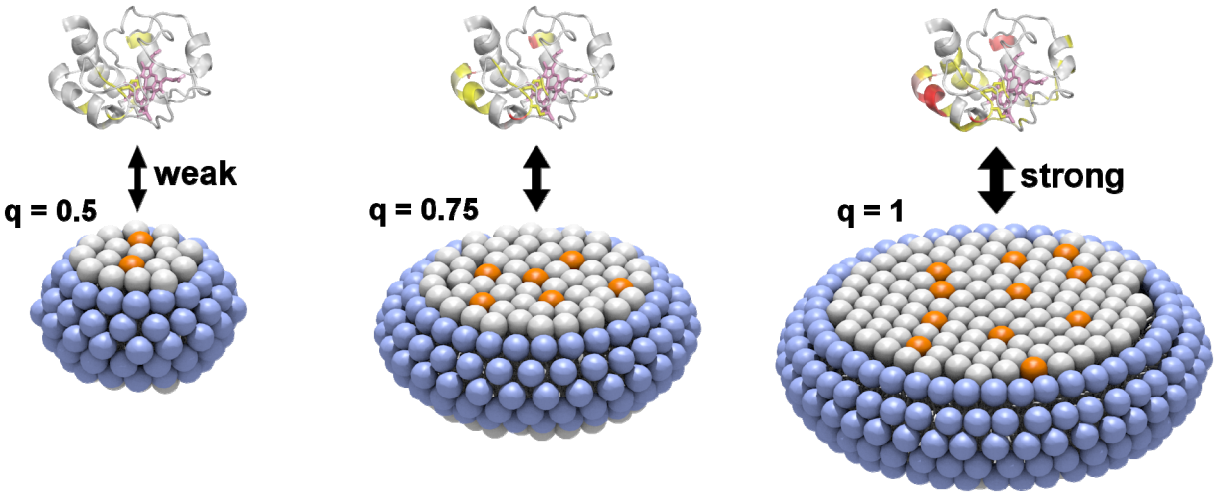

Fig. S5. Schematic diagram of the interaction between cyt *c* and CL-containing bicelles. The head groups of lipid molecules are shown as sphere models. The colors of the residues in the protein structure (PDB:1AKK) are the same as those in Fig. 3. DHPC, DMPC, and CL molecules are shown in blue, gray, and orange, respectively.

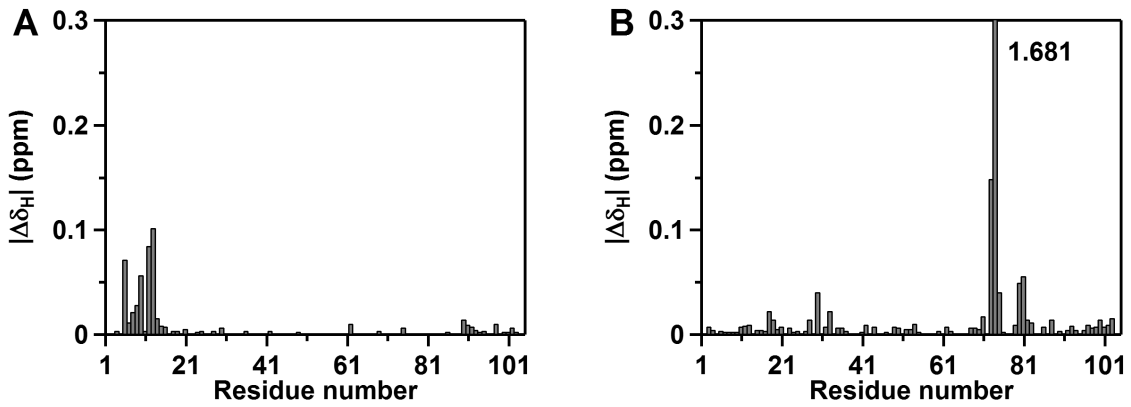

Fig. S6. Differences between the ^{1}H chemical shifts of backbone NMR signals of oxidized WT and mutant cyt *c*: (A) between WT and K8A cyt *c* and (B) between WT and K72A cyt *c*. The differences induced by the mutations are represented in bar graphs. Measurement conditions: solution condition; 25 mM HEPES-NaOH, pH 6.8, containing 50 mM NaCl; [cyt *c*], 0.3 mM; [$K_3[Fe(CN)_6]$], 0.3 mM; temperature, 25 ºC.

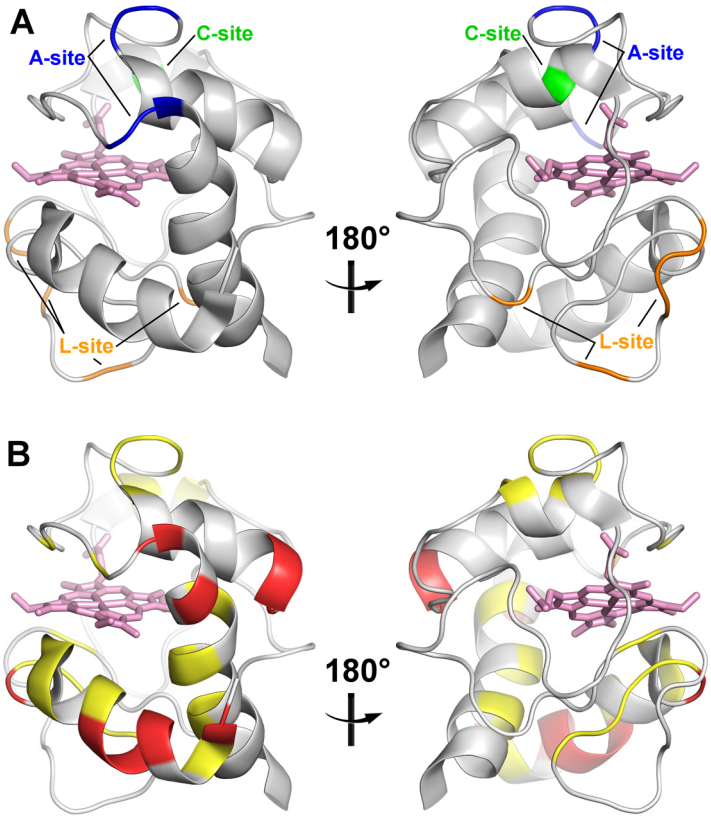

Fig. S7. Mapping of the amino acid residues of cyt *c*. (A) The proposed CL-interaction sites and (B) the residues with substantial CSP values. The protein structure (PDB:1AKK) is shown as a ribbon model. The residues of the A-, C-, and L-sites are shown in blue, green, and orange, respectively. The residues with the CSP values of $x < 0.008$, $0.008 \leqq x < 0.014$, and $0.014 \leqq x$ are shown in gray, yellow, and red, respectively. The heme is shown as a stick model in pink. The left and right figures are rotated horizontally 180º.

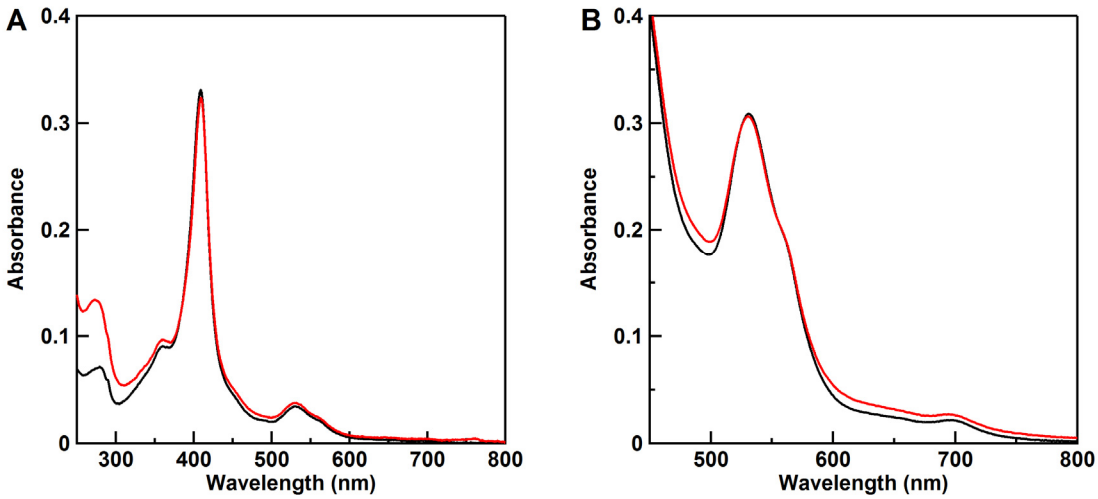

Fig. S8. Optical absorption spectra of oxidized WT cyt *c*: (A) 250-800 nm and (B) 450-800 nm regions. The spectra of WT cyt *c* in the absence (black) and presence (red) of CL-containing q=1 bicelles. Measurement conditions: solution condition; 25 mM HEPES-NaOH, pH 6.8, containing 50 mM NaCl; [cyt *c*], 0.3 mM; [DHPC], 30 mM; [DMPC], 27 mM; [CL], 3 mM; [$K_3[Fe(CN)_6]$], 0.3 mM; path-length, (A) 0.1 mm and (B) 1 mm; temperature, 25 ºC.

Table S1. ^{31}P NMR signal linewidths of CL-containing bicelles and ^{1}H-^{15}N HSQC NMR signal linewidths of oxidized WT cyt *c* in the presence and absence of CL-containing bicelles.

NMR signal	full width at half maximum (Hz)			
bicelle	q=1	q=0.75	q=0.5	
DHPC (^{31}P)	3.3 ± 0.7	1.9 ± 0.2	1.3 ± 0.2	
DMPC (^{31}P)	5.8 ± 0.3	3.3 ± 0.1	1.9 ± 0.1	
CL (^{31}P)	5.5 ± 0.5	4.0 ± 0.5	2.7 ± 0.5	
	presence of the bicelles			absence of the bicelles
WT cyt *c*[a]	q=1	q=0.75	q=0.5	
backbone NH (^{1}H)	31.3 ± 12.3	23.3 ± 4.4	20.5 ± 4.1	20.9 ± 3.7
backbone NH (^{15}N)	14.5 ± 2.9	11.2 ± 1.5	9.3 ± 1.4	8.7 ± 1.3

[a] Average linewidths of the observed HSQC signals.

Table S2. Nucleotide sequences of the primers.

Primer	Sequence[a]
#1-F	GTTCAGAAGTGTGCCCAGTGCCACACCGTTGAAAAGG
#1-R	AAAAATCTTCTTGCCTTTCTCAACATCACCC
#2-F	TCACTTACACAGATGCCAATAAGAACAAAGGCATCATCTGG
#2-R	ATCCAGGGGCCTGACCTGTCTTC
#3-F	CCTGGAAAGAGGAAACACTGATGGAGTATTTGGAGAATCCC
#3-R	TGATGCCTTTGTTCTTATTGGCATCTGTG
#4-F	AGAAAGGGAAGACTTAATAGCTTATCTCAAAAAAGCTACTAATG
#4-R	GTCTTCTTCTTAATGCCAGCAAAGATCATTTTTGTTCCAGGGATG
HH-K8A-F	GCGATTTTTGTTCAGAAGTGTGCCCAGTGC
HH-K8A-R	CTTGCCTTTCTCAACATCACCCAT
HH-K72A-F	GCGAAGTACATCCCTGGAACAA
HH-K72A-R	GGGATTCTCCAAATACTCCATCAGTG

[a] Underlines indicate the replaced nucleotides.

References

[1] P. P. Parui, M. S. Deshpande, S. Nagao, H. Kamikubo, H. Komori, Y. Higuchi, M. Kataoka, S. Hirota, *Biochemistry* **2013**, *52*, 8732-8744.

[2] A. S. Morar, D. Kakouras, G. B. Young, J. Boyd, G. J. Pielak, *J. Biol. Inorg. Chem.* **1999**, *4*, 220-222.

[3] E. A. Berry, B. L. Trumpower, *Anal. Biochem.* **1987**, *161*, 1-15.

[4] F. Delaglio, S. Grzesiek, G. W. Vuister, G. Zhu, J. Pfeifer, A. Bax, *J. Biomol. NMR* **1995**, *6*, 277-293.

[5] M. P. Williamson, *Prog. Nucl. Magn. Reson. Spectrosc.* **2013**, *73*, 1-16.